

Deep learning model for ECG reconstruction reveals the information content of ECG leads.

Tomasz Gradowski, Teodor Buchner

^aWarsaw University of Technology, Faculty of Physics, Koszykowa
75, Warsaw, 00662, Poland

Abstract

This study introduces a deep learning model based on the U-net architecture to reconstruct missing leads in electrocardiograms (ECGs). Using publicly available datasets, the model was trained to regenerate 12-lead ECG data from reduced lead configurations, demonstrating high accuracy in lead reconstruction. The results highlight the ability of the model to quantify the information content of each ECG lead and their inter-lead correlations. This has significant implications for optimizing lead selection in diagnostic scenarios, particularly in settings where full 12-lead ECGs are impractical. Additionally, the study provides insights into the physiological underpinnings of ECG signals and their propagation. The findings pave the way for advancements in telemedicine, portable ECG devices, and personalized cardiac diagnostics by reducing redundancy and enhancing signal interpretation.

Keywords: ECG, deep learning, U-net, reconstruction

1. Introduction

The electrocardiogram (ECG) is a widely used diagnostic tool in cardiology. It is a non-invasive method to record the electrical activity of the heart. The standard ECG consists of 12 leads, which are recorded from different positions on the body. Each lead provides a different view of the electrical activity of the heart, and the combination of all leads gives a comprehensive picture of the heart's function. However, in some cases, not all leads are available, either due to technical limitations or due to the patient's condition. Furthermore, reducing a number of leads reduces patient burden and device complexity and therefore improves the availability of ECG equipment, and the quality of the data [1], which defines a clear design target [2]. In such

cases, it is desirable to be able to reconstruct the missing leads from the available leads. However, apart from this technical motivation, an information theory aspect is also interesting.

So far, many methods have been used to determine the information content of electrodes. Linear correlation is the most obvious method [3, 4, 5], which also enables detecting electrode reversal [6] and allows evaluating the possibilities of regeneration of 12 leads from a custom reduced electrode set, such as proprietary EASI [4] or corrected orthogonal leads [3]. A correlation matrix may be obtained, either by classical correlation [5] or with the use of dedicated Deep Neural Networks (DNN) [7], which allows one to study the extent of overlap between the data provided by various electrodes. Electrodes of a minimal degree of overlap are considered the most important for ventricular arrhythmia detection [7]. The huge capabilities provided by modern neural networks also allow reconstruction of missing data either between electrodes or between time segments [8]. However, it has long been known that correlation, or lack thereof, is the idea of paramount importance to vectorcardiography, which was historically based on the initial assumption that the limb and the precordial leads represent projection onto various directions in the frontal and transverse planes, respectively. The idea of validation of the current reference point for precordial leads - the Wilson central terminal [9, 10], determination of an optimum reference point [11] verification of added value delivered either by vectorcardiography alone [12] or by its specific representations [13] easily follows.

Modern DNNs present a unique opportunity to study not only simple linear correlations but also the true added value of the information content between various electrode setups. It is important to understand that each of the correlations observed in the ECG stems from physical relations present in the large, spatially extended source, i.e., the heart.

The first point of the analysis is the analysis of limb leads: only two of them are statistically independent, as $I + III = II$. Does it really mean that, in the spatial direction of lead II, we observe combined activity from two other spatial directions: lead I and lead III? The same relations are obtained for Goldberger augmented leads, a linear combination of limb leads. Therefore, lead III and augmented leads are excluded from further analysis, as the relationship between them will be strong and directly follow their definition.

The second point is the relationship between the limb leads and the precordial leads. Here, the situation is more subtle, as we actually observe a

mirror effect of composed limb leads, which is reflected in precordial leads, to which it serves as a reference. The analysis of mirror patterns has a long tradition [14, 15], but it is also studied in a contemporary context [16, 17].

The third point concerns the interrelations between precordial leads. Due to the small distance between electrodes, the difference in signal is not so large, and a clear gradual change of QRS polarity is visible [18] is a manifestation of a clear correlation between neighboring electrodes. Electrical shunting by excessive amounts of electrode gel is a common mistake, which completely abolishes the observed changes [19].

Anyway, this short resume shows that various relations that concern the information content of ECG leads are known and that the utilization of DNN allows the extension of the statistical models far beyond the Pearson correlation coefficient. Apart from motivation from basic science, many practical aspects were already mentioned: an ability to reduce the electrode set or vice versa, to utilize over-completeness of the ECG to cover missing spatiotemporal segments, and last but not least, to determine the electrodes that are crucial from the point of view of arrhythmia analysis. It is important to note that due to its bipolar nature, the ECG does represent only spatial gradient, which is only a difference between much stronger unipolar signals. Therefore, care must be taken to maximize the information carried by this signal, which represents the asymmetry of cardiogenic electromagnetic wave [20].

This study presents a deep learning model to reconstruct missing ECG leads. The model is based on the U-net architecture [21], which is effective for image segmentation tasks. We train the model on a large dataset of ECG recordings and evaluate its performance on a separate validation dataset. We show that the model can reconstruct missing leads and that the reconstruction quality depends on the source leads.

A key advantage of the model is that it can estimate the amount of information carried by each lead and the correlations between leads. This information can be useful for understanding the heart’s underlying physiology and improving the accuracy of ECG interpretation.

The remainder of the paper is organized as follows. In Section 2, we describe the methods used in the study. In Section 3, we present the results of the study. In Section 4, we discuss the results and their implications. Finally, in Section 5, we present our conclusions and suggest directions for future work.

2. Methods

2.1. Model

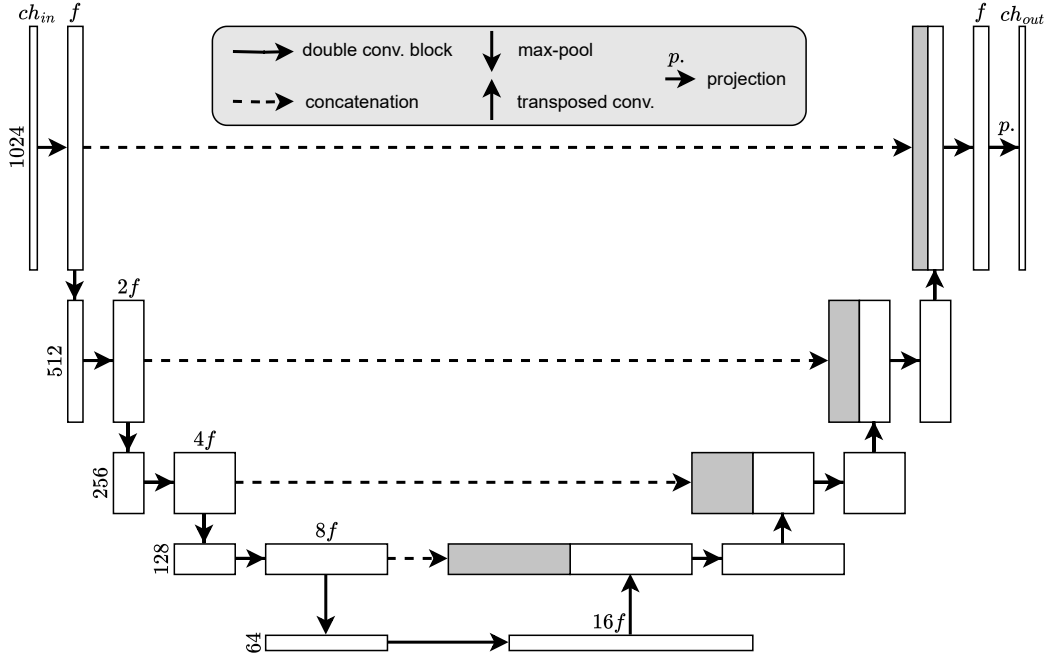


Figure 1: U-net architecture adopted for ECG reconstruction. Rectangular blocks represent tensors with dimensions shown at the top (number of channels) and on the left (number of samples). In our model, the initial number of channels $f = 64$ was used. ch_{in} and ch_{out} represent the number of input and output leads, respectively.

The model used in this study is based on the U-net architecture [21], which consists of an encoder-decoder network with skip connections between the corresponding layers of the encoder and decoder. The encoder part of the network consists of a series of convolutional and max-pooling layers that down-sample the input data. The decoder part of the network consists of a series of convolutional and upsampling layers, which upsample the data to the original resolution. The skip connections between the encoder and decoder layers allow the network to capture both local and global features of the input data.

We implemented the model as close as possible to the original U-net architecture, with some modifications to adapt it to the ECG reconstruction task (Fig.1). The model consists of an encoder with four convolutional blocks

(*conv-blocks*), one conv-block in the bottleneck, and a decoder with four conv-blocks. Each convolutional block consists of two layers with a kernel size of 3, a stride of 1, and padding of 1, followed by a batch normalization layer and a ReLU activation function. The dropout layers, present in the original U-net architecture, were removed from our model for simplicity. The change of the feature maps’ depth is done by the first convolutional layer of each block. The downsampling in the encoder is done by max-pooling layers with a kernel size of 2 and a stride of 2. Transposed convolutional layers do the upsampling in the decoder with a kernel size of 2 and a stride of 2. The final layer of the network is a convolutional layer with a kernel size of 1 for the projection of the feature maps to the number of leads to be reconstructed. There is no activation function in the final layer.

The model takes a set of ECG leads as input and outputs a set of reconstructed leads. The input leads are encoded as a 2D array, where the rows correspond to the time samples, and the columns correspond to the leads. The output leads are also encoded as a 2D array, with the same number of rows as the input leads and a variable number of columns depending on the number of leads to be reconstructed. The length of the input and output leads is set to 1024 samples (8192 ms).

The model is trained using a dataset of ECG recordings. The model is trained to reconstruct missing leads. The loss function used for training is the mean squared error (MSE) between the reconstructed leads and the ground truth. The model is trained for 100 epochs using the AdamW optimizer with a learning rate of $3 \cdot 10^{-4}$ and a batch size of 32.

To perform the study, we trained 25 models with different sets of input leads: 3 models with single limb lead (I, II, III) as input, 1 model with 2 limb leads (I, II) as input, 6 models with 2 limb leads (I, II) and 1 chest (precordial) lead (V1, V2, V3, V4, V5, V6) as input, and 15 models with 2 limb leads (I, II) and all possible combinations of 2 chest leads as input.

In all cases, the model was trained to reconstruct all the precordial leads that were not present in the set of input leads.

2.2. Data

The data used in this study come from two separate datasets, one for training and validation and one for testing. The training and validation sets were based on the PTB-XL dataset [22, 23], a large publicly available electrocardiography dataset. The dataset contains 21799 12-lead ECG recordings from 18869 patients. The recordings were sampled at 500 Hz and had a

duration of 10 seconds. For the purpose of this study, we downsampled the recordings to 125 Hz and truncated them to 1024 samples (8192 ms). The dataset was split into a training set and a validation set, with 90% of the recordings used for training and 10% used for validation. The testing dataset was based on the PTB dataset [24] is a publicly available dataset of 549 12-lead ECG recordings from 290 patients. The recordings were sampled at 1000 Hz, varying from 30 to 120 seconds. For the purpose of this study, we downsampled the recordings to 125 Hz and split them into 1024 samples (8192 ms) segments, getting 7061 segments in total. PTB-XL and PTB datasets are available from the PhysioNet platform [25].

3. Results

In this section, we present the results of the study. We show the performance of the model on the testing dataset. Our model is, in fact, a set of models, each trained with a different set of input leads. We evaluated the performance of each model by calculating the Pearson correlation coefficient (PCC), which measures the linear correlation between the reconstructed leads and the ground truth. PCC is much easier to interpret than the MSE used as the loss function during the training, as it's value is bounded between -1 and 1. We also show the reconstructed leads for selected examples.

The results are presented in two groups. The first group consists of models trained with one limb lead as input (I, II, III), two limb leads as input (I, II), and two limb leads and one precordial lead as input (I, II, Vx). The second group consists of models trained with two limb leads and two precordial leads as input (I, II, Vx, Vy). In each group, we show the results for selected examples.

Fig. 2 shows the results of the models in the first group. The first three rows show the results of the models trained with one limb lead as input. The fourth row shows the results of the model trained with two limb leads as input. We excluded the model trained with all three limb leads as input, as the leads are linearly dependent ($I + III = II$), and the third lead does not carry any additional information.

A set of plots of input and reconstructed leads for the I+II and I+II+V3 models is shown in Fig. 3-6. Signals with PCC values close to the average PCC of all signals for a particular model were selected to show the typical performance of the model. The primary source of error in the reconstruction is the T wave, which is the most volatile part of the ECG signal. The model

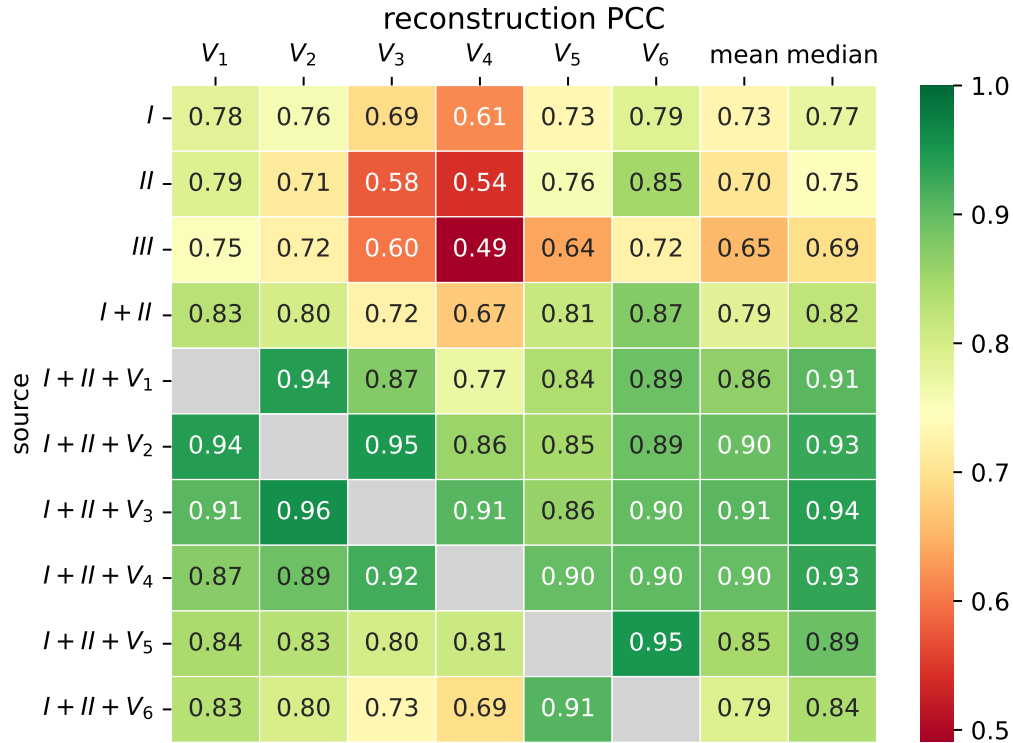


Figure 2: Performance of the models trained with single limb leads as input (*I*, *II*, *III*), two limb leads as input (*I*, *II*), and two limb leads and one precordial lead as input (*I*, *II*, V_x). The table shows the mean PCC between the reconstructed leads and the ground truth for each model. Mean and median PCC values for the testing dataset are shown at the most right columns.

struggles with reconstructing the amplitudes of R waves, possibly due to the low resolution of the input data (125 Hz) and the low impact of the R wave on the loss function due to its width.

Fig. 7 shows the results of the models trained with two limb leads and two precordial leads as input. Each combination of two precordial leads was examined. In this group, we observed significantly better reconstruction of the precordial leads than in the first group. The plots of the input and reconstructed leads for the selected model (*I+II+V₂+V₄*) are shown in Fig. 8 for a selected example with a PCC value close to the average PCC of all signals for this model.

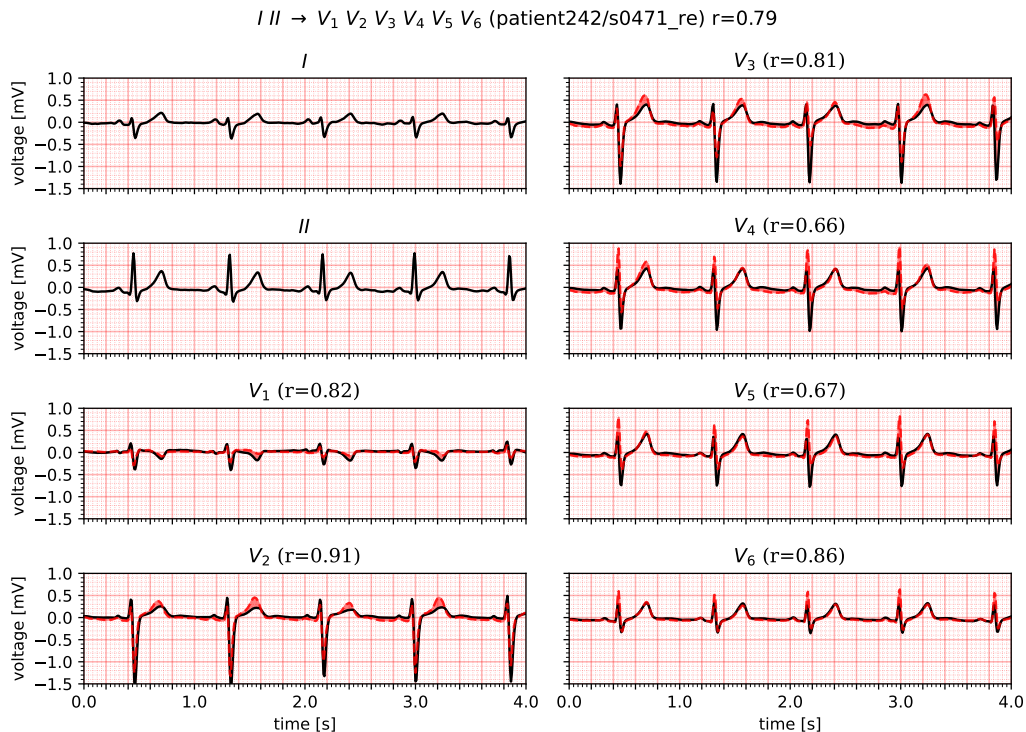


Figure 3: Patient #242, female, 28 years old, healthy control. Reconstruction of precordial leads from the set of limb leads (I, II), exemplary ECG recording from the PTB dataset with the PCC value close to the average PCC of all signals for this model. Black solid lines represent the real signal; red dashed lines represent the reconstructed signal, and the difference between them is filled with a light red. The PCC value for each reconstructed lead is shown at the top of the subplot. Only the first 4 seconds of the signal are shown.

4. Discussion

First, let us discuss the results of the single-lead models. In these models, we take only one limb lead as input and try to reconstruct all the precordial leads. The quality of the reconstruction can be interpreted as the measure of the correlation between the input lead and the precordial leads. We must remember that all precordial leads have the same reference point, the Wilson central terminal, so the information from all the limb electrodes is present in all precordial leads to some extent. However, by comparing the results of the single-lead models, we can try to estimate the correlation between the single electrodes as well.

The results show that leads V1 and V6 are reconstructed with the highest

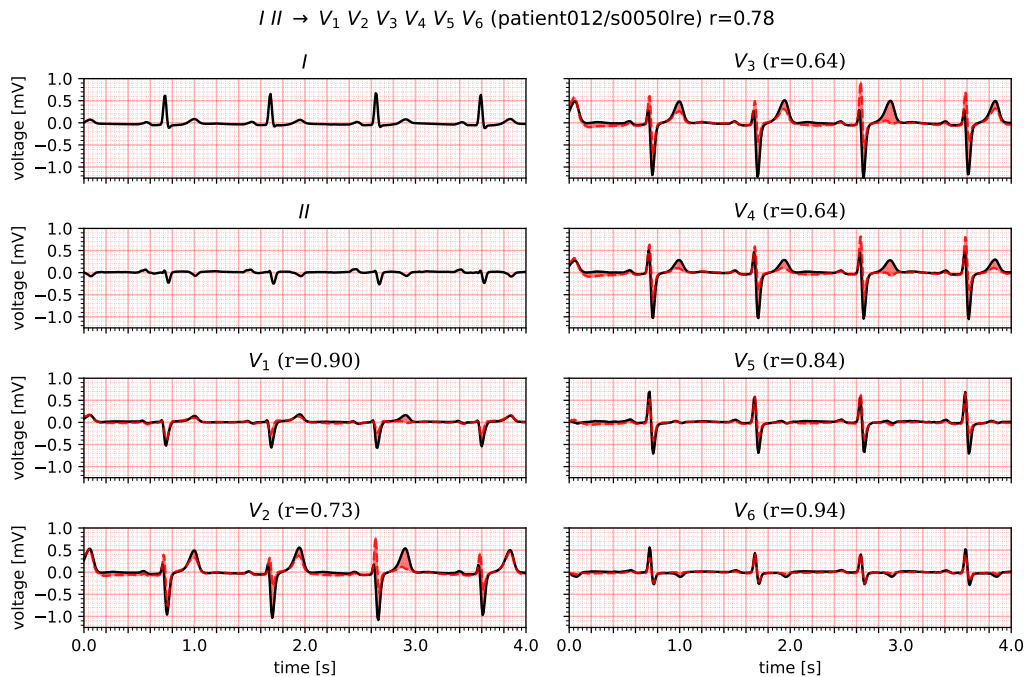


Figure 4: Patient #012, male, 67 years old, reason for admission: myocardial infarction. See Fig. 3 caption for details.

accuracy in all three scenarios (Fig. 2, first three rows). In particular, lead V6 appears to be more closely correlated with limb leads II and I. A slightly better reconstruction of V6 from lead II than from lead I suggests a stronger correlation between the potential on the V6 electrode and the potential on the LL electrode (left leg) than LA (left arm), since the electrode potential RA (right arm) is present in both leads I and II.

The V3 and V4 leads were reconstructed with the lowest accuracy in all three scenarios (V4 has the lowest PCC value, V3 has the highest MSE value). This suggests that the potential on the V3 and V4 electrodes carries information that is not present in the limb leads. This is consistent with the fact that V3 is placed closest to the interventricular septum and is, on average, equally susceptible to potentials from both ventricles. Since it is centrally located on the chest, it captures a unique combination of signals that are not as prominent on the limb leads. The significance of the V3 lead will be seen in the 3-lead models.

To estimate the correlation between precordial leads, we trained models

with two limb leads and one precordial lead as input ($I + II + V_x$). We also trained a model with two limb leads ($I+II$) as input, which serves as a baseline for the comparison.

The first observation is that precordial leads are the most correlated with the closest precordial leads, e.g., including the V2 lead in the input leads results in significantly better reconstruction of the V1 and V3 leads. This is very intuitive since the precordial electrodes are placed in a line along the heart’s axis, and the potential of one electrode is expected to be the most correlated with the potentials of the adjacent electrodes.

The results show that the reconstruction of the precordial leads is the best when the V3 lead is used as input. This confirms the previous observation that the V3 lead carries the most information about the heart’s electrical activity, which is not present in the limb leads. The worst reconstruction is obtained when the V6 lead is used as an input. This observation is consistent with the previous one that the V6 lead is the most correlated with the limb leads and carries the least additional information. Including the V6 lead in the input leads does not affect the reconstruction of the V1-V4 leads and improves the reconstruction of only the V5 lead, measured from the closest electrode to the V6 electrode.

The following models assume a scenario where we want to reconstruct all the precordial leads from two limb leads and two precordial leads. This scenario is possible in a clinical setting, where precordial leads are unavailable due to the patient’s condition or technical limitations. A performant model in this scenario would open the way for the development of a portable ECG device with fewer leads, which could be used in emergencies or remote areas. The decision on which ECG leads to include in such a device would be based on the correlation between the leads and the quality of the reconstruction. The PCC analysis gives us very close results with no decisive winner in this category. We show the combination $I + II + V2 + V4$ in Fig. 8, as it got the lowest MSE value. Leads V2 and V4 are positioned over areas central to the electrical activity of the heart. V2 is placed in the fourth intercostal space at the left sternal border, while V4 is placed in the fifth intercostal space at the midclavicular line. The proximity of these leads to critical cardiac structures allows them to capture significant electrical activity from both the anterior and septal regions of the heart. V2 and V4 provide a balanced view of the heart’s electrical activity; V2 captures data from the right ventricle and the septal area, while V4 captures signals from the anterior wall of the left ventricle. This complementary information is crucial for accurately reconstructing

the missing leads. Although adjacent leads (like V2 and V3) provide highly correlated data, they can introduce redundancy rather than additional useful information. V2 and V4, being slightly more spatially separated, offer diverse and non-redundant information that enhances reconstruction accuracy.

5. Conclusion

The results of this study are promising and show the potential of deep learning models for the reconstruction of ECG. The method for estimating the amount of information carried by each lead and the correlations between the leads may be significant from the clinical point of view.

First, the proposed method can optimize ECG use. By quantifying the information carried by each lead, clinicians can prioritize specific leads over others. This can be especially useful when a full 12-lead ECG is impractical, such as in remote monitoring or emergency situations. Streamlining lead selection could improve diagnostic efficiency without compromising accuracy.

Second, the method can reduce redundancy. Correlations between leads can reveal which ones provide redundant information. By identifying this redundancy, clinicians can reduce the number of leads used in specific scenarios, potentially simplifying the equipment, reducing patient discomfort, and shortening ECG reading times.

Third, the method can improve personalized diagnostics. Different patients may have varying degrees of information spread across ECG leads. The presented method can help tailor the interpretation of the ECG to individual patients. It can also help detect subtle cardiac abnormalities.

Another value of the method is that it can provide a better understanding of cardiac physiology. Understanding the correlations between leads can provide deeper insight into the electrical activity of the heart and how it propagates across different axes, potentially aiding in a more accurate localization of ischemic or arrhythmic areas.

Finally, the method can improve telemedicine. For remote health monitoring, using fewer leads without sacrificing the quality of information could be a game changer. It could make ECG monitoring more accessible and affordable, especially in low-resource settings.

These advances can lead to faster diagnosis, more targeted treatment, and potentially lower healthcare costs.

References

- [1] H. Yoo, Y. Yum, Y. Kim, J.-H. Kim, H.-J. Park, H. J. Joo, Restoration of missing or low-quality 12-lead ecg signals using ensemble deep-learning model with optimal combination, *Biomedical Signal Processing and Control* 83 (2023) 104690. doi:10.1016/j.bspc.2023.104690. URL <http://dx.doi.org/10.1016/j.bspc.2023.104690>
- [2] J. Xue, Does a reduced ecg lead set contain the full 12-lead ecg information for interpretation, in: 2024 Computing in Cardiology Conference (CinC), Vol. 51 of CinC2024, Computing in Cardiology, 2024. doi:10.22489/cinc.2024.473. URL <http://dx.doi.org/10.22489/CinC.2024.473>
- [3] H. V. Pipberger, S. M. Bialek, J. K. Perloff, H. W. Schnaper, Correlation of clinical information in the standard 12-lead ECG and in a corrected orthogonal 3-lead ECG, *Am. Heart J.* 61 (1) (1961) 34–43.
- [4] M. Holderith, T. Schanze, Cross-Correlation based comparison between the conventional 12-lead ECG and an EASI derived 12-lead ECG, *Curr. Dir. Biomed. Eng.* 4 (1) (2018) 621–624.
- [5] U. Jain, A. Butchy, M. Leasure, V. Covalesky, D. McCormick, G. Mintz, Redundancy and novelty between ECG leads based on linear correlation, in: Proceedings of the 16th International Joint Conference on Biomedical Engineering Systems and Technologies, SCITEPRESS - Science and Technology Publications, 2023, pp. 359–365.
- [6] I. Jekova, V. Krasteva, R. Leber, R. Schmid, R. Twerenbold, C. Müller, T. Reichlin, R. Abächerli, Inter-lead correlation analysis for automated detection of cable reversals in 12/16-lead ECG, *Comput. Methods Programs Biomed.* 134 (2016) 31–41.
- [7] C. Zhang, J. Li, S. Pang, F. Xu, S. Zhou, A 12-lead ECG correlation network model exploring the inter-lead relationships, *EPL* 140 (3) (2022) 31001.
- [8] A. Lence, A. Fall, F. Granese, B. Hanczar, J.-E. Salem, J.-D. Zucker, E. Prifti, ECGrecover: A deep learning approach for electrocardiogram signal completion, *arXiv* (2024). arXiv:2406.16901.

- [9] G. D. Gargiulo, True unipolar ECG machine for wilson central terminal measurements, *Biomed Res. Int.* 2015 (2015) 586397.
- [10] G. Gargiulo, P. Bifulco, M. Cesarelli, A. McEwan, A. OLoughlin, J. Tapsen, A. Thiagalingam, The wilson’s central terminal (WCT): A systematic error in ECG recordings, *Heart Lung Circ.* 25 (2016) S263.
- [11] H. Moeinzadeh, P. Bifulco, M. Cesarelli, A. L. McEwan, A. O’Loughlin, I. M. Shugman, J. C. Tapsen, A. Thiagalingam, G. D. Gargiulo, Minimization of the wilson’s central terminal voltage potential via a genetic algorithm, *BMC Res. Notes* 11 (1) (Dec. 2018).
- [12] S. Man, A. C. Maan, M. J. Schaliq, C. A. Swenne, Vectorcardiographic diagnostic & prognostic information derived from the 12-lead electrocardiogram: Historical review and clinical perspective, *J. Electrocardiol.* 48 (4) (2015) 463–475.
- [13] M. J. Boonstra, D. H. Brooks, P. Loh, P. M. van Dam, CineECG: A novel method to image the average activation sequence in the heart from the 12-lead ECG, *Comput. Biol. Med.* 141 (105128) (2022) 105128.
- [14] O. H. Schmitt, R. B. Levine, E. Simonson, Electrocardiographic mirror pattern studies. I, *Am. Heart J.* 45 (3) (1953) 416–428.
- [15] D. A. Brody, G. D. Copeland, Electrocardiographic cancellation: Some observations concerning the “nondipolar” fraction of precordial electrocardiograms, *Am. Heart J.* 56 (3) (1958) 381–395.
- [16] G. N. Vaidya, S. Antoine, S. H. Imam, H. Kozman, H. Smulyan, D. Villarreal, Reciprocal ST-segment changes in myocardial infarction: Ischemia at distance versus mirror reflection of ST-elevation, *Am. J. Med. Sci.* 355 (2) (2018) 162–167.
- [17] J. Wang, J. Li, S. Diao, H. Xu, F. Ding, Atypical de winter ECG pattern may be the mirror image of ST elevation, *Ann. Noninvasive Electrocardiol.* 27 (3) (2022) e12915.
- [18] S. Meek, ABC of clinical electrocardiography: Introduction. II—Basic terminology, *BMJ* 324 (7335) (2002) 470–473.

- [19] A. R. Pérez-Riera, R. Barbosa-Barros, R. Daminello-Raimundo, L. C. de Abreu, Main artifacts in electrocardiography, *Ann. Noninvasive Electrocardiol.* 23 (2) (2018) e12494.
- [20] T. Buchner, M. Zajdel, K. Peęczalski, P. Nowak, Finite velocity of ECG signal propagation: preliminary theory, results of a pilot experiment and consequences for medical diagnosis, *Sci. Rep.* 13 (1) (2023) 4716.
- [21] O. Ronneberger, P. Fischer, T. Brox, U-net: Convolutional networks for biomedical image segmentation, in: N. Navab, J. Hornegger, W. M. Wells, A. F. Frangi (Eds.), *Medical Image Computing and Computer-Assisted Intervention – MICCAI 2015*, Springer International Publishing, Cham, 2015, pp. 234–241.
- [22] P. Wagner, N. Strodthoff, R.-D. Bousseljot, W. Samek, T. Schaeffter, PTB-XL, a large publicly available electrocardiography dataset (2022).
- [23] P. Wagner, N. Strodthoff, R.-D. Bousseljot, D. Kreiseler, F. I. Lunze, W. Samek, T. Schaeffter, PTB-XL, a large publicly available electrocardiography dataset, *Sci. Data* 7 (1) (2020) 154.
- [24] R.-D. Bousseljot, D. Kreiseler, A. Schnabel, The PTB diagnostic ECG database (2004).
- [25] A. L. Goldberger, L. A. Amaral, L. Glass, J. M. Hausdorff, P. C. Ivanov, R. G. Mark, J. E. Mietus, G. B. Moody, C. K. Peng, H. E. Stanley, PhysioBank, PhysioToolkit, and PhysioNet: components of a new research resource for complex physiologic signals, *Circulation* 101 (23) (2000) E215–20.



Figure 5: Patient #203, male, 32 years old. Reason for admission: bundle branch block. Reconstruction of precordial leads from the set of limb leads (I, II) and V₃ lead. See Fig. 3 caption for details.



Figure 6: Patient #232, female, 70 years old. Reason for admission: Cardiomyopathy. Bundle branch block diagnosed. Reconstruction of precordial leads from the set of limb leads (I, II) and V3 lead. See Fig. 3 caption for details.

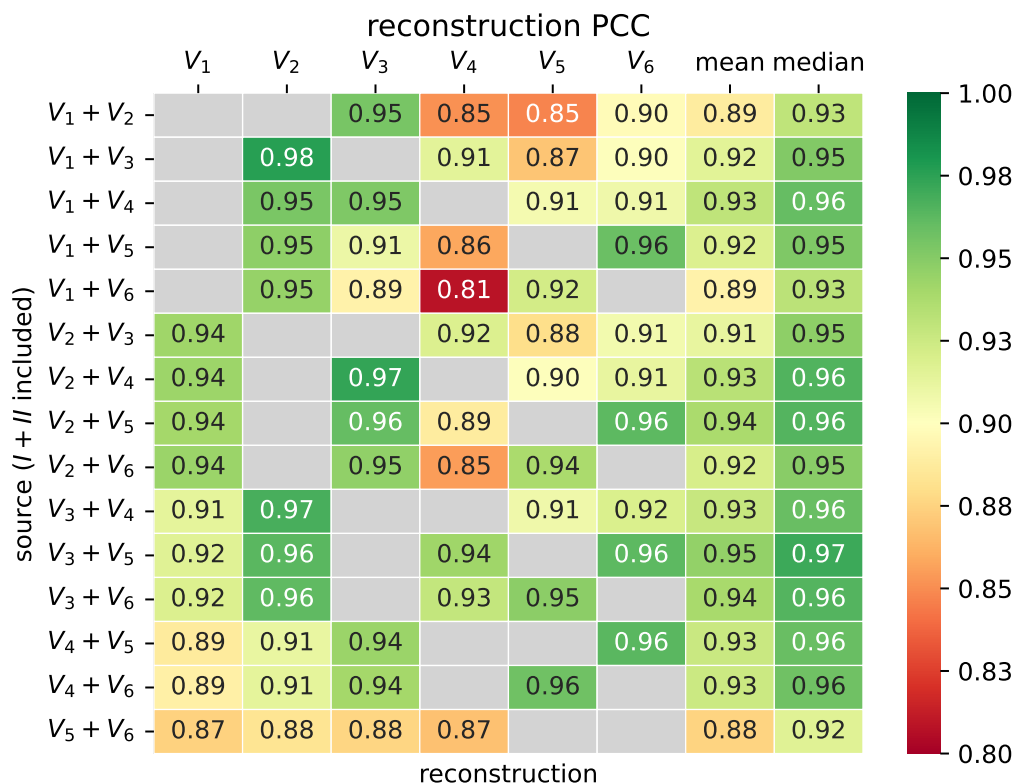


Figure 7: Performance of the models trained with two limb leads (I, II) and two precordial leads as input. The table shows the mean PCC between the reconstructed leads and the ground truth for each model. Mean and median PCC values for the testing dataset are shown at the most right columns.

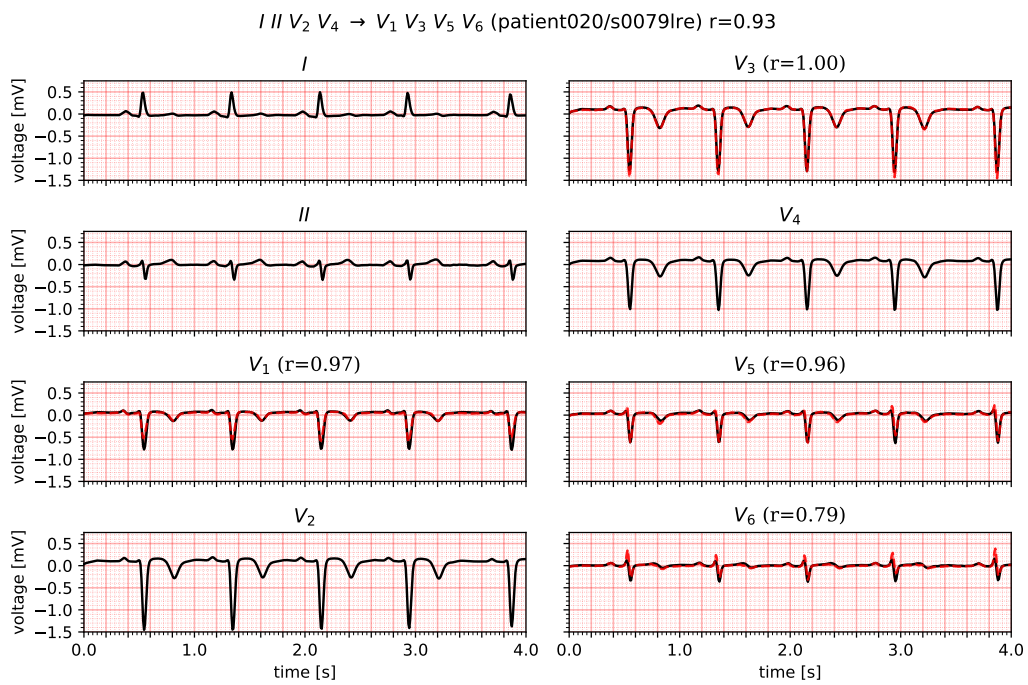


Figure 8: Patient #020, female, 54 years old. Reason for admission: Myocardial infarction.